Surface & Coatings Technology xxx (2016) xxx–xxx

Contents lists available at ScienceDirect

Surface & Coatings Technology

journal homepage: www.elsevier.com/locate/surfcoat

# Mechanical properties of austenitic stainless steel treated by active screen plasma nitriding

Yasuhiro Hoshiyama [a,*], Ryoji Mizobata [b], Hidekazu Miyake [a]

[a] Department of Chemistry and Materials Engineering, Faculty of Chemistry, Materials and Bioengineering, Kansai University, 3-3-35 Yamatecho, Suita, Osaka 564-8680, Japan
[b] Graduate School of Science and Engineering, Kansai University, 3-3-35 Yamatecho, Suita, Osaka 564-8680, Japan

ARTICLE INFO

*Article history:*
Received 30 October 2015
Revised 8 April 2016
Accepted in revised form 11 July 2016
Available online xxxx

*Keywords:*
Active screen
Plasma nitriding
Mechanical property
Austenitic stainless steel

ABSTRACT

In the active screen plasma nitiriding method, the materials to be processed are insulated and a voltage is applied to a metallic and basket-shaped mesh screen installed around the material as the cathode and the furnace wall as the anode. In this research, we subjected austenitic stainless steel to active screen plasma nitiriding treatments and evaluated the mechanical properties of the treated samples. Active screen plasma nitiriding experiments were carried out using a direct current plasma-nitriding unit. Nitriding treatments were performed in a nitrogen-hydrogen atmosphere for 7.2–28.8 ks at 673 K. The S-phase formed on the surface of the nitrided samples. The thickness of the S-phase increased with increasing treatment time. The hardness of the nitrided samples increased with increasing treatment time. The wear resistance and fatigue strength of austenitic stainless steel were improved by active-screen plasma nitriding.



## 1. Introduction

As austenitic stainless steel exhibits superior corrosion resistance, it is used in diverse fields, such as household goods and automobile parts; however, austenitic stainless steel also exhibits low hardness and poor wear resistance and its use as a structural material is limited. The plasma nitriding method is commonly used to improve the mechanical properties of austenitic stainless steel. In the nitriding method, the surface of the material to be processed is cleaned by a sputtering action of mixed nitrogen and hydrogen gas. Therefore, this method enables the nitridization of stainless steel, which has been considered to be difficult because it is covered with a passivation film, without any specific pretreatment. Nonetheless, the plasma nitriding method may lead to some problems: the edging effect, wherein electrical discharge is concentrated on the edges and projections of processed materials; arcing, wherein the form of electrical discharge instantly changes, creating an electric arc; and the hollow cathode effect, wherein the areas of electrical discharge overlap. To address these problems, the active screen plasma nitriding (ASPN) method was developed [1–11]. In the ASPN method, the materials to be processed are insulated and a voltage is applied to a metallic and basket-shaped mesh screen installed around the material as the cathode and the furnace wall as the anode. In this manner, nitrogen is diffused into the sample; i.e., glow discharge is generated between the furnace wall and the screen instead of the surface of the processed material. The plasma formed on the screen surface contains nitrogen molecules, atoms, ions, and electrons, along with constituent atoms of the screen and their nitride. The nitride formed on the screen is transported to the surface of the processed material via gas flow in the furnace, and nitrogen atoms diffuse into the processed material; therefore, the edging effect, arcing, and hollow cathode effect do not occur. Attempts have been made to evaluate hardness and wear resistance of ASPN-treated austenitic stainless steel [2,5,6]. However, little information has been reported regarding the evaluation of fatigue strength and tensile strength of ASPN-treated austenitic stainless steel. In this study, we performed ASPN on austenitic stainless steel (AISI304) and evaluated its mechanical properties.

## 2. Experimental part

We used AISI304 austenitic stainless steel as the experimental material: both planar (length: 20 mm, width: 10 mm, and thickness: 5 mm) and cylindrical (length of the parallel portion: 25 mm, diameter of the parallel portion: 8 mm) samples with a diameter of 15 mm were prepared. AISI304 mesh was processed to prepare two screens. ASPN experiments were carried out using a direct current plasma-nitriding unit (NDK, Japan, JIN-1S). Fig. 1 shows schematics of the ASPN

* Corresponding author at: Kansai University, 3-3-35 Yamatecho, Suita, Osaka 564-8680, Japan.
*E-mail address:* hosiyama@kansai-u.ac.jp (Y. Hoshiyama).

http://dx.doi.org/10.1016/j.surfcoat.2016.07.032
0257-8972/

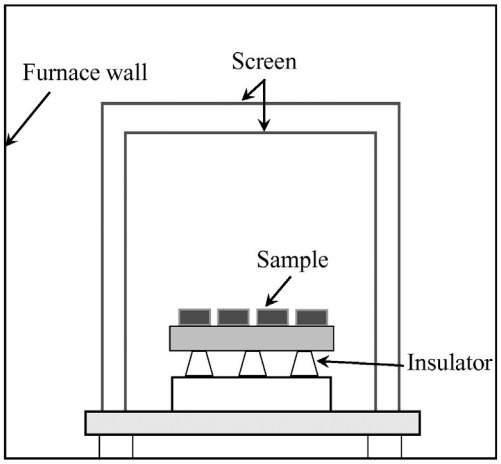


**Fig. 1.** Schematics of the ASPN equipment.

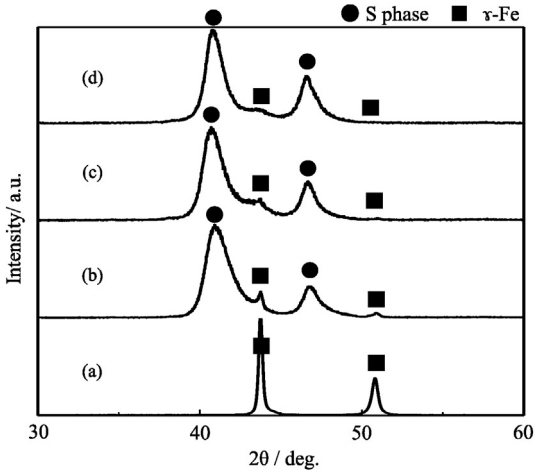


**Fig. 2.** X-ray diffraction pattern of the planar sample after the ASPN treatment.

equipment. In the case of the planar sample, a base made of AISI304 was placed on the sample stage in the furnace and a porcelain crucible was placed on this base to insulate the sample. A petri dish made of AISI304 was used as a cover. Samples were placed on the petri dish at equal intervals, and a screen (170 mm in diameter and 220 mm in height) was used to cover the samples, with the distance between the sample and the top of the screen being 170 mm. Furthermore, to cover this screen, a screen with a diameter of 190 mm and height of 225 mm was placed on the sample stage. Cylindrical samples were placed in a vertical placement method onto a petri dish and processed such that the distance between the sample and the screen was even. A screen 170 mm in diameter and 220 mm in height was placed on the sample such that the distance between the upper part of the sample and the top of the screen was 25 mm. Furthermore, to cover this screen, another screen with a diameter of 190 mm and height of 225 mm was placed on the sample stage. For the ASPN treatment, the concentration ratio of $N_2$ and $H_2$ was set as 1:1 and the treatment was conducted at a temperature and pressure of 673 K and 100 Pa, respectively. The treatment duration was 7.2–28.8 ks. For the samples treated by ASPN, cross-sectional structure observations (JEOL, Japan, JSM-6060LV), glow discharge spectrometry (GDS; HORIBA, Japan, GD-Profiler 2) analyses, X-ray diffraction (RIGAKU, Japan, RINT-2550V) analyses, Vickers microhardness (Matsuzawa, Japan, MXT50) tests (load: 0.1 N), Suga abrasion (Suga Test Instruments, Japan, NUS-ISO-3) tests (abrasion material: SiC sandpaper #1000), tensile (Shimadzu, Japan, UH-F50A) tests, and Ono-type rotating bending fatigue (Shimadzu, Japan, H-6) tests (rotational speed: 3400 rpm) were performed.

## 3. Results and discussion

Fig. 2 shows the X-ray diffraction pattern of the planar sample after the ASPN treatment. The diffraction peak in the pattern of the samples subjected to ASPN treatment shifted to lower angles compared to that in the pattern of the non-treated sample. All ASPN-treated samples exhibited diffraction peaks attributable to the S-phase, which is believed to be a supersaturated solid solution of nitrogen in austenite fcc structure [12–15]. As the nitriding time increases, the intensity of the diffraction peaks of the mother phase (i.e., the austenite phase) becomes relatively weak. This decrease in intensity is attributable to more nitrogen forming a solid solution with the sample with increasing nitriding time, thereby, causing the nitriding layer to thicken. In addition, the diffraction peak of the S-phase in the patterns of the samples subjected to ASPN treatment shifted to lower angles with increasing treatment time. This shift was due to a large amount of nitrogen forming a solid solution in the 14.4 ks and 28.8 ks samples compared to that in the 7.2 ks sample. Fig. 3 shows cross-sectional scanning electron microscope (SEM) images of ASPN-treated planar samples. In all of the ASPN-treated samples, a layer different from the mother phase was confirmed to form on the surface of the samples. On the basis of the X-ray diffraction patterns in Fig. 2, this layer is a nitriding layer comprising the S-phase. The thickness of the S-phase of the planar and cylindrical samples are listed in Table 1. The thickness of these layers on the ASPN-treated planar samples was approximately 2.4 μm, 4.0 μm, and 5.8 μm for the 7.2 ks-, 14.4 ks-, and 28.8 ks-ASPN-treated samples, respectively. With the increased time of the ASPN treatment, the thickness of the S-phase became thicker. On the basis of these results, we hypothesized that the longer ASPN treatment times result in deeper inward diffusion of nitrogen, resulting in a thicker S-phase. The thickness of the S-phase at the parallel portion of the cylindrical ASPN-treated sample was approximately 2.2 μm, 4.6 μm, and 6.2 μm for the 7.2 ks-, 14.4 ks-, and 28.8 ks-ASPN-treated samples, respectively. The thickness of the S-phase varied within the range from 0.2 μm to 0.6 μm between the ASPN-treated planar and cylindrical samples. This variation is due to the difference in the position of the samples and the different distances between the screen and the sample for cylindrical and planar samples. In the case of the cylindrical samples, irrespective of the treatment time, the S-phase became thicker in the order of the upper, middle, and lower portions. In addition, the S-phase became thicker with increasing ASPN treatment time in all portions (upper, middle, and lower) in the cylindrical sample. The ASPN treatment insulated the sample to be processed, and the nitride formed on the screen was deposited onto the sample surface via gas flow in the furnace; then, nitrogen was diffused through this process. Nitriding gas flows from the top to bottom of the nitriding furnace used in these experiments; therefore, if the distance between the sample surface and the screen becomes larger, nitride deposition on the sample becomes difficult. This difficulty led to the thickening of the S-phase in the order of the upper, middle, and lower portions. These results indicate that, when the ASPN treatment is applied to a sample with a large height, the treatment conditions must be adjusted to ensure that the thickness of the S-phase is uniform. Fig. 4 shows the GDS measurement results for the ASPN-treated planar samples. The nitrogen concentration was high up to 2.5 μm, 4.2 μm, and 6.5 μm in the samples subjected to the ASPN process for 7.2 ks, 14.4 ks, and 28.8 ks, respectively. These results correspond to the thickness of the nitriding layer shown in the cross-sectional SEM images in Fig. 3. Fig. 5 shows the results of Vickers microhardness tests of the ASPN-treated planar samples. As the ASPN treatment time increased, the hardness increased, because of the increased thickness of the nitriding layer

Please cite this article as: Y. Hoshiyama, et al., Surf. Coat. Technol. (2016), http://dx.doi.org/10.1016/j.surfcoat.2016.07.032